Contents lists available at ScienceDirect

Progress in Organic Coatings

journal homepage: www.elsevier.com

Macromolecular aggregation and electrochemical behavior of pyrrolyl-, anilynyl- and thiophenyl-silicon compounds as precursors for thin hybrid films

Giulia Conchetto, Cristina M. Santi, Monica Trueba*, Stefano P. Trasatti

Department of Chemistry, Università degli Studi di Milano, Via Golgi 19, 20133 Milan, Italy

ARTICLE INFO

Keywords:
Silicon-organic hybrid precursors
Electrochemistry
Semiconducting behavior

ABSTRACT

Aniline, pyrrole and thiophene substituted with methoxysilyl propyl side chains were investigated by means of spectroscopic and electrochemical techniques. The effect of hydrolysis and ex-situ irradiation of solutions prepared in different solvent mixtures, containing either methanol or methylacetate in excess, was considered also. The development of stable intermediate species in solution is governed by intramolecular polarization of the hydrolyzed monomer rather than by ex-situ photoxidation or electro-oxidation of the monomer head group. Cooperative non-covalent OH-π interactions between the electron deficient silanol (SiOH) and the electron rich aromatic π system leading to mixed- n-p type redox behavior of the hybrid films are confirmed for the case of N-substituted pyrrolyl-silicon derivative. Less efficient interactions of the more basic N-AnSi derivative result from the deprotonation and self-condensation of SiOH, being supported by the prevalent p-type charge transport of the related hybrid film. For the case thiophenyl-silicon derivatives, charge trapping manifesting n-type redox behavior dominates for the case of α-substituted thiophene rather than for the parent β-substituted derivative but with jellification, indicating effective OH-π stabilization of σ-coupled α,α' dimer structures by a short-range intramolecular mechanism. The establishment and modulation of constructive OH-π interactions determine the macromolecular aggregation and redox behavior of the hybrid films. The diverse properties exhibited by the hybrid precursors support different protection mechanisms against corrosion.

1. Introduction

The integration of silane chemistry in the development of composite conducting polymer films is of significant general interest. Application areas include electronic and optical materials [1], sensors and biosensors [2], bioimplants [3,4], electroresponsive hydrogels [5], electronic textiles [6], protective coatings [7], among other. Silanes functionalized with monomers of conducting polymers such as aniline, pyrrole and thiophene as hybrid precursors at a molecular level have attracted less attention.

From our studies with pyrrolyl- and anilynyl-silicon compounds (Fig. 1a,b) for surface treatment of Al alloys [8–15], both silane chemistry and conducting polymers (electro)chemistry determine the mechanism and the extent of corrosion inhibition [8–12]. The formation of OH-π stabilized $\alpha - \alpha'$ linked pyrrole (Py) oligomers in solution and the charge pinning action of silanol (SiOH) leading to n-type semiconductivity of the chemically-deposited hybrid film [15] have been supported by experimental studies using the neat non-hydrolyzed monomer [14], as theoretically predicted [13]. The n-type charge transpor justifies the good barrier action against localized corrosion by favoring O_2 reduction reaction at the film/solution interface while the penetration of aggressive Cl^- is hindered [8,9]. The p-type semiconductivity [15] for the case of anilynyl-silicon precursor supports the more defective hybrid network at a molecular level. Nonetheless, passivity recovery and inhibition of microgalvanic corrosion are effective due to aniline acid-base redox processes and metallo-complexation [10–12]. Local acid-based reactions in a constrained reaction environment has been indicated further by the formation of MgO mesocrystals with (111) preferential orientation [16] rather than $Mg(OH)_2$ as main corrosion products of treated AM60B Mg alloy (Fig. 2a,b) (unpublished results). This is strengthened by the fact that Mg^{2+} complexation by aniline is negligible as compared to other metal ions like Cu^{2+}, Cu^{+} and Fe^{3+} [12]. Significant inhibition of mild steel corrosion by surface treatment with thiophenyl-silicon precursors has been indicated also (Fig. 2c,d) (unpublished results). In similarity with pyrrole derivative,

* Corresponding author.
Email address: monica.trueba@unimi.it (M. Trueba)

https://doi.org/10.1016/j.porgcoat.2018.05.010
Received 18 December 2017; Received in revised form 17 April 2018; Accepted 7 May 2018
Available online xxx
0300-9440/

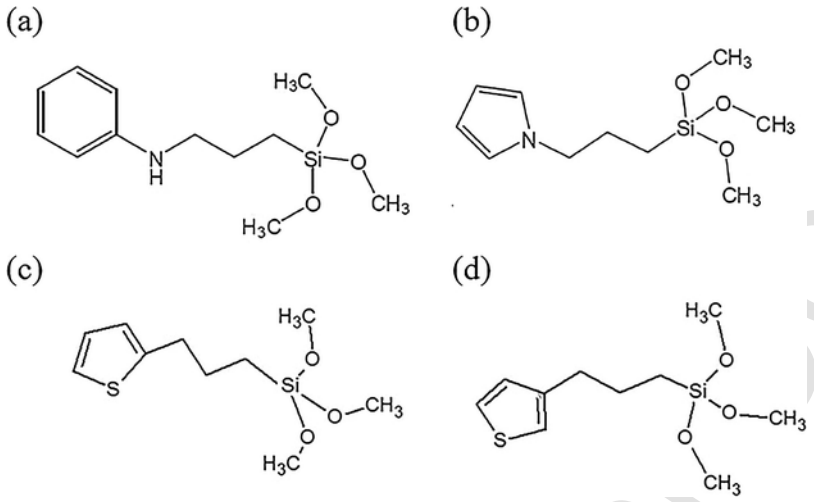

Fig. 1. Schematic structures of hybrid monomers: (a) N-(3-trimethoxysilyl propyl) aniline (N-AnSi), (b) N-(3-trimethoxysilyl propyl) pyrrole (N-PySi), (c) α-(3-trimethoxysilyl propyl) thiophene (α-TphSi), (d) β-(3-trimethoxysilyl propyl) thiophene (β-TphSi).

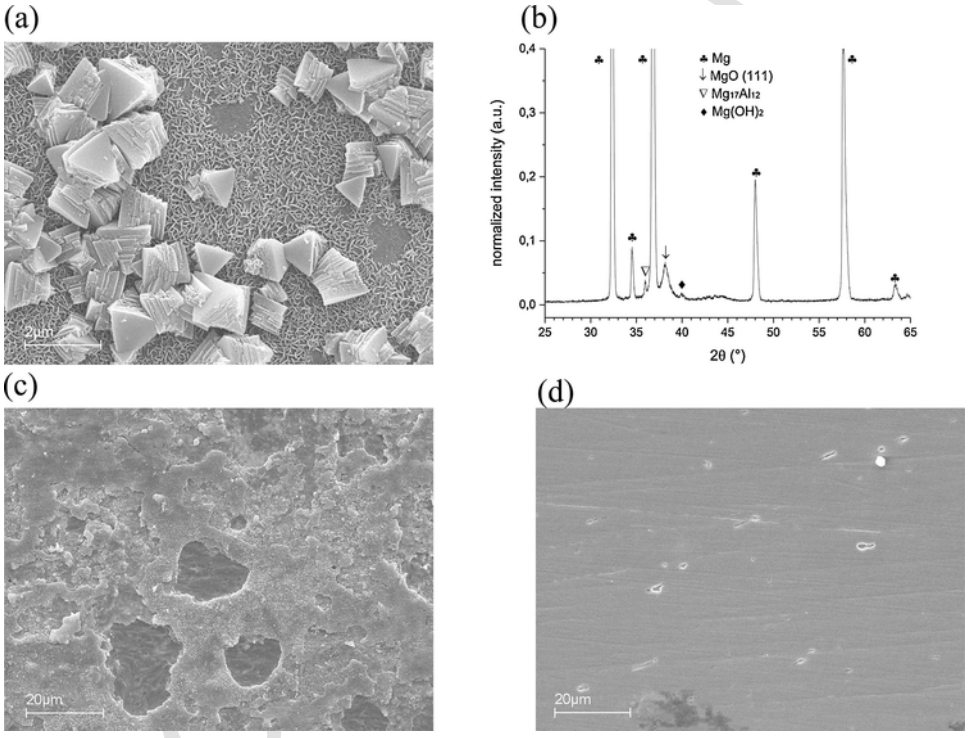

Fig. 2. (a,b) Surface SEM image and the relative XRD spectrum of coated AM60B Mg alloy with N-AnSi hybrid film after 8 days of exposure in 0.1 M NaCl at 30 °C; (c,d) Surface SEM images of bare and treated with α-(3-(trimethoxysilyl)propylthio) thiophene mild steel after 8 days of exposure in 0.1 M NaCl at 30 °C.

the semiconducting behavior of the thiophene-based hybrid film could determine the barrier action against metal degradation. The investigation of the mechanism of macromolecular aggregation of these silicon-organic hybrid precursors in condensed and solid state phases, as well as of the intrinsic redox behavior of the hybrid films, is indispensable for further understanding of the mechanism of protection against corrosion [8–12] and for the design of advanced coatings with specific functions.

In this work, the aggregation in condensed phase of anilynyl-, pyrrolyl- and thiophenyl-silicon hybrid monomers (Fig. 1a–d), and the electrochemical behavior of the electrogrown hybrid networks on inert substrates, are investigated by means of spectroscopic and electrochemical techniques. Factors such as the extent of hydrolysis in methanol-based solutions and of ex-situ photo-oxidation are considered. Hydrolyzed precursors in solutions containing methylacetate in excess, this solvent being low VOC, non-HAP and biodegradable, were studied in parallel.

2. Experimental part

2.1. Test solutions

The hybrid monomers, namely N-[3-(trimethoxysilyl) propyl] aniline (N-AnSi, Fig. 1a), N-[3-(trimethoxysilyl) propyl] pyrrole (N-PySi, Fig. 1b), α-(3-trimethoxysilylpropyl)thiophene (α-ThpSi, Fig. 1c) were used as received (>98%, Fluorochem, Sigma Aldrich). The non-commercially available β-(3-trimethoxysilylpropyl)thiophene (β-ThpSi, Fig. 1d) was synthesized ad-hoc following a two-step synthetic route (Sup-

plementary data) [17]. The compound was immediately used as such in the experiments after checking its purity by ^{1}H NMR to minimize decomposition processes by hydrolysis. The test solutions were prepared at 4 vol% by adding 400 µL of a given hybrid monomer to 10 mL of solvent mixtures made of methanol and water (MeOH/H_2O 95:5) or of methyl acetate, ethanol and water (MeOAc/EtOH/H_2O 50:25:25), using commercially available reagent grade organic solvents and water of quality MilliQ. The pH was adjusted to 4 by adding acetic acid. For sake of simplicity, a given test solution is designated in the following as analyte(solvent), where the analyte identifies the hybrid monomer and the solvent that present in excess in the solvent mixture, i.e. MeOH or MeOAc.

A given analyte(solvent) solution was left under stagnant conditions during different times (aging time, t_{aging}) such as to promote chemical reactions that involve methoxy groups hydrolysis, hydrogen bonding and self-condensation of silanol groups, as well as the possible formation of conjugated species due to intramolecular polarization of the hydrolyzed analyte [9–12]. Another set of either as-prepared ($t_{aging} = 0$ h) or aged analyte(solvent) solutions was consecutively exposed to controlled polychromatic irradiation (white light) during increasing time periods of 5 h each (t_{irrad}) using a Newport lamp 450 W with maximum excitation range between 400 and 700 nm. An aliquot of 200 µL of aged and/or consecutively irradiated analyte(solvent) solution was placed in a glass cuvette containing 3.5 mL of a given solvent mixture. The visible spectra (320 and 900 nm) with a spectral resolution of 2 nm were recorded using a spectrophotometer Hach DR 3900. Base line corrections were made with a reagent blank of analyte-free solvent mixture.

2.2. Cyclic voltammetry

A single compartment three-electrode glass cell with a capacity of 5 mL was used. The supporting electrolyte was 0.1 M tetrabutilammonium perchlorate in acetonitrile (TBAP/MeCN). Unless otherwise indicated, the working electrode was glassy carbon (GC) with geometrical surface area of 0.7 cm^2 (Ø = 3 mm, AMEL). Before use, the surface was polished with diamond paste (0.25 µm) on a cloth impregnated with acetone. Pt wire and Ag/AgCl/$KCl_{(sat.)}$ (+0.200 V vs SHE) were used as counter and reference electrodes, respectively. The latter was connected to the test solution via a salt bridge containing 0.1 M TBAP/MeCN. The electrochemical system was connected to a computer-driven Solartron 1286 potentiostat.

Cyclic voltammetry experiments were performed at room temperature under stagnant conditions. A volume of 200 µL of a given analyte(solvent) solution, either as-prepared (hybrid monomer concentration of about 10^{-2}M), hydrolyzed (t_{aging}) or irradiated (t_{irrad}), was added to 3.5 mL of 0.1 M TBAP/MeCN. Unless otherwise indicated, electropolymerization was carried out by recurrent potential cycling between 0 and + 1.2 V (at least 3 cycles) at a scan rate of 100 mV/s. Similarly, the redox behavior of the as-deposited films was investigated by consecutive potential cycling between + 1.2 and − 1.2 V in monomer-free 0.1 M TBAP/MeCN.

In order to check for a possible effect of the solvent mixtures on the electrode potential, the cyclic voltammograms of 1 mg of ferrocene in monomer-free 0.1 M TBAP/MeCN containing 200 µL of a given solvent mixture were recorded. The redox potential of the ferrocene/ferrocinium (Fc^+|Fc) couple, which electronic energy transfer is supposed to be independent of the working solvent [18], was of +0.41 ± 0.02 V with respect to Ag/AgCl/$KCl_{(sat.)}$ for all testing conditions. Accordingly, the electrode potentials as being determined by MeCN in excess were not corrected and are referred in the text to the Ag/AgCl/$KCl_{(sat.)}$ reference electrode.

2.3. Spectro-electrochemical experiments

These experiments were carried out to investigate the soluble oligomers produced during electro-oxidation of α-ThpSi(MeOH) (Fig. 1c). A three-electrode UV–vis-NIR spectroelectrochemical thin-layer quartz glass cell (1.0 mm optical path) for conducting static experiments (SEC-C, ALS Co. Ltd, Japan) was employed. A given amount of α-ThpSi(MeOH), either as prepared or aged up to 14 days was added to 0.1 M TBAP/MeCN supporting electrolyte. The three-electrode system consisted in a Pt mesh as working electrode, a Pt wire as counter electrode and Ag/AgCl/$KCl_{(sat.)}$ as reference electrode. This was connected through a salt bridge containing the supporting electrolyte solution.

The cell was placed in the sample holder of a UV-3600 Plus UV–vis-NIR spectrophotometer (Schimadzu) with three detectors (a photomultiplier tube for the ultraviolet and visible regions and InGaAs and cooled PbS detectors for the near-infrared region), operating in the wavelength range of 185–3300 nm and with 0.1 nm of resolution. The electrodes were connected to an external Gamry Ref600 potentiostat. UV–vis-NIR spectra were collected consecutively during anodic polarization from +0.0 V to +2.0 V at a scan rate of 2 mV/s and thereafter corrected by subtraction of similarly recorded spectra using the analyte-free 0.1 M TBAP/MeCN (background electrolyte).

3. Results and discussions

3.1. Electronic properties of the hybrid monomers and oligomers in solution

N-PySi solutions progressively developed an orange brown coloration with ex-situ irradiation (t_{irrad}) and with aging (t_{aging}), regardless the nature of the main solvent (MeOH or MeOAc). No sediments or precipitates were formed in any case. The coloration was always less intense for the case of the solvent mixture containing MeOAc in excess due to limited hydrolysis in this polar but aprotic solvent, and thus less favored formation of OH-π agglomerates. Typical spectra are shown in Fig. 3a,b for as-prepared and 7-days aged solutions after prolonged irradiation. Although the intensity of the absorption features was always smaller for the case of N-PySi(MeOAc), the position of the peaks along the wavelength (λ) axe did not change with either t_{irrad} or t_{aging}. For a given initial test condition, the peaks at 450 and 490 nm were more intense for the case of aged N-PySi(MeOH) (Fig. 3a), whereas the shoulder at 430 nm was always pronounced for N-PySi(MeOAc) (Fig. 3b). No bands were detected at $\lambda > 600$ nm, thus indicating hindered coupling for chain growth with the prevalent formation of small α − α' linked Py oligomers [19]. Note that no oxidant was purposely added to the solutions, while hydrolysis of methoxy groups —OCH_3, hydrogen bonding between silanol groups SiOH and their self-condensation to form linear siloxane linkages (Si-O-Si) [9,13] may proceed during the time of exposure to white light also. Based on previous UV–vis results with Py(MeOH) and N-PySi(MeOH) as a function of aging (up to one month) during exposure to natural light [9], the peak at 490 nm appears to be characteristic of hydrolyzed α − α' Py-linked oligomeric structures. From the plots of the peaks intensity as a function of t_{irrad} (Fig. 3c,d), the absorbance of the peaks at 450 and 490 nm increases linearly with photo-oxidation regardless the nature of the solvent in excess and t_{aging}, whereas that of the peak at 585 nm changes little. This supports the prevalent accumulation of short oligomeric structures with photo-oxidation, being more significant for the case of polar and protic MeOH in excess and the corresponding aged solution ($t_{aging} = 7$ days, Fig. 3c) despite the fact that the mobility of charge carriers should decrease with hydrolysis and possible self-condensation of SiOH. Nonetheless, the similar trends of the absorption peaks indicates that the oligomeriza-

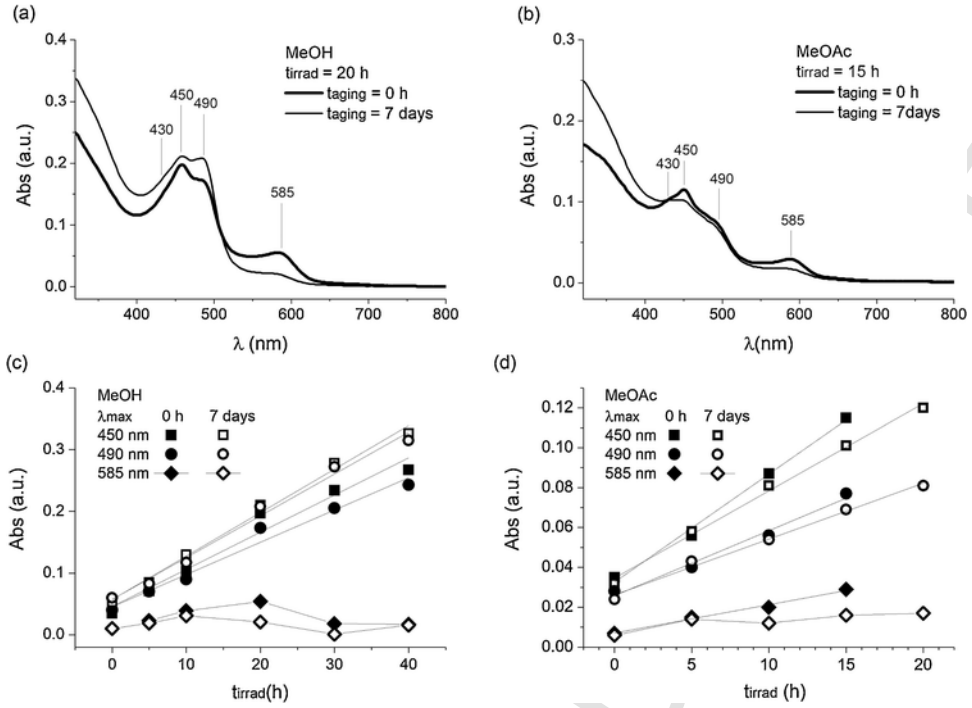

Fig. 3. (a,b) Visible spectra of as-prepared and 7-days aged N-PySi(MeOH) and N-PySi(MeOAc) solutions after consecutive ex-situ irradiation; (c,d) plots of the intensity of the main absorption peaks as a function of the irradiation time.

tion mechanism via α − α' coupling of Py rings prevails. That is, structurally similar oligomeric structures develop in both solvent mixtures but the extent of hydrolysis determine the amount of hydrolyzed oligomeric domains in condensed phase. The 450- and 490-nm peaks are thus ascribed to aromatic and quinoid α − α' Py segments, being more favored in the case of N-PySi(MeOH) due to intramolecular polarization effects [13]. The feature at 430 nm corresponds to non-hydrolyzed or partially hydrolyzed aromatic Py structures. The results support the instauration of non-covalent OH-π stabilizing interactions between the electron deficient silanol (SiOH) and the electron-rich π system of Py ring [13], limiting the self-condensation of SiOH [8,9] and favoring the charge trapping [14].

The solutions of N-AnSi(MeOH) acquired a pink coloration which turned cherry red with t_{aging}. The color change correlated with the detection of a shoulder at 570 nm in addition to the 490-nm peak (pink solution) (Fig. 4a), reproducing previous results [9,10,12]. The peak at

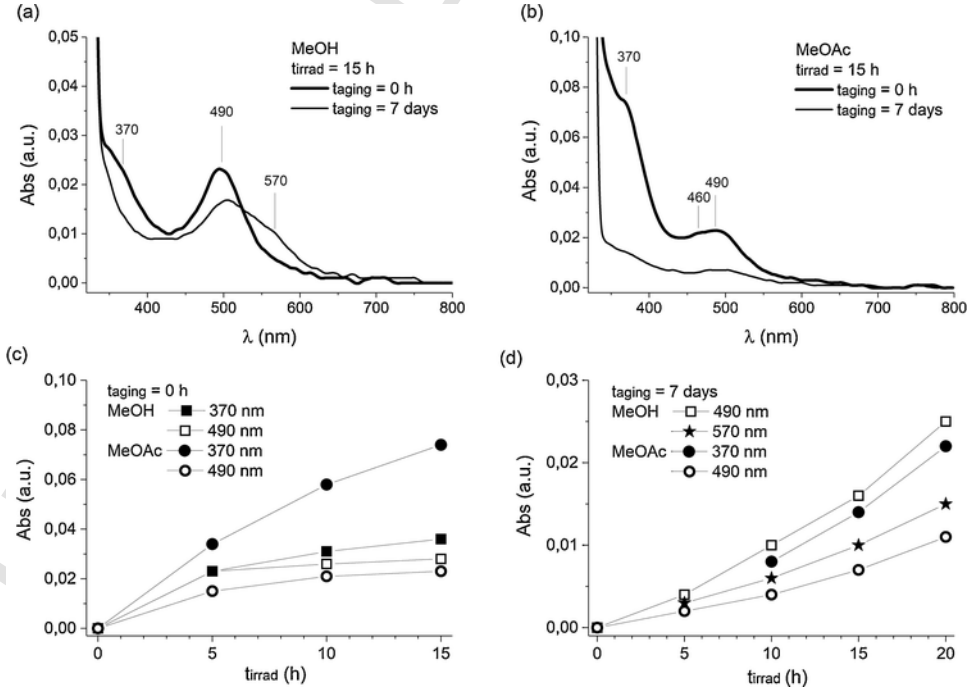

Fig. 4. (a,b) Visible spectra of as-prepared and 7-days aged N-AnSi(MeOH) and N-AnSi(MeOAc) solutions after consecutive ex-situ irradiation; (c,d) plots of the intensity of the main absorption peaks as a function of the irradiation time.

490 nm is ascribed to nitrenium radical cations $NH^{\bullet+}$ stabilized as zwitterions $[C_6H_5NH^{\bullet+}(CH_2)_3Si(O^-)(OH)_2]$ (mononegative silanol group). The fast hydrolysis of methoxy groups (75% of completion after about 3 h [11]) facilitates self-condensation of SiOH leading to linear and tridimensional Si-O-Si linkages [9]. Thus, radicals coupling to form semiquinoid (SQ) aniline structures (570-nm peak) is promoted with aging. This is supported by the spectra obtained for N-AnSi(MeOAc) (Fig. 4b), showing a more intense shoulder at 370 nm in addition to a shoulder at 460 nm. Alternated benzenoid/quinoid (B-Q) oligomeric structures of aniline coexist with stable nitrenium radical cations (490 nm). These absorption features decrease similarly while no new peaks emerge with aging. Accordingly, structurally different oligomeric domains involving the aniline head group develops in the presence of polar but aprotic MeOAc. Differently from pyrrole, the lone pair of electrons on N atom of aniline are delocalized but not involved in the aromatization. Thus, N-AnSi is more basic and thus more prone for bonding a proton, but hydrogen bonded O···H—N complexes through the deprotonation of SiOH are destabilized with aging due to the latter species self-condensation and formation of three-dimensional siloxane linkages [9–12]. This is supported by the similar trends of the variation of the intensity of the most relevant and common to both solvent mixtures absorption features with t_{irrad} for a given initial aging condition (Fig. 4c,d). That is, for $t_{aging} = 0$ h (Fig. 4c), the intensity of the peak at 490 nm increases markedly only after 5 h of ex-situ irradiation, regardless the nature of the solvent in excess. Photoxidation of hydrolyzed monomer and small oligomers is facilitated as charge screening by SiOH decreases with aging (Fig. 4d). Note that, for the case of MeOH in excess, the peak at 570 nm increases as that at 490 nm, in support to the prevalent formation of semiquinoid hybrid agglomerates [12].

Opposite to N-PySi and N-AnSi, the thiophenyl-silicon compounds (Fig. 1c,d) developed no color in solution, regardless the nature of the solvent in excess, the extent of ex-situ irradiation (up to 15 h) and of aging (up to 7 days). It is to be noticed that the Cα of the thiophene ring are free in the case of β-ThpSi (Fig. 1d), as for N-PySi (Fig. 1a). Also, the inductive effect of the alkyl side chain is expected to be similar for all the investigated monomers (Fig. 1). Accordingly, no intramolecular polarization favoring the formation of conjugated oligomeric species is indicated for the case of thiophene derivatives, being ascribed to the different reactivity of the monomer head group: aniline > pyrrole > thiophene [20]. As noticed before, the lone pair of electrons on N of Py ring are part of the aromatic sextet. This is also the case of thiophene but the second lone pair of electrons of S may bond to a proton or other electrophile without disrupting the aromatic system. However, the higher resonance energy of thiophene makes this monomer less reactive.

3.2. Electrogrowth and solid state processes of N-PySi and N-AnSi hybrid films

Thin films of N-PySi and N-AnSi were electrodeposited by recurrent potential cycling (up to 3 cycles) from as-prepared, ex-situ irradiated and/or aged analyte(solvent) solutions, using 0.1 M TBAP/MeCN as background electrolyte. For the case of N-PySi, the electrochemical behavior resembled very much that of neat N-PySi in 0.1 M TBAP/MeCN on a Pt electrode [14]. The current increased importantly at E > +0.8 V while broad anodic and cathodic redox waves between +0.2 and +0.9 V emerged with subsequent cycling, as illustrated in Fig. 5 for selected conditions. An anodic shoulder at about +0.4 V was always detected and became more pronounced with aging rather than with ex-situ photo-oxidation of N-PySi(MeOH) (Fig. 5a). This highlights further the importance of OH-π interactions and the charge pinning action of SiOH that call for participation of electrolyte cations $TBAP^+$ for charge compensation, thus obtaining mixed n-p type redox behavior [13,14]. These observations are strengthened by the voltammograms of the films deposited using N-PySi(MeOAc) (Fig. 5b). The redox bands are more intense and change little with t_{irrad} for a given initial aging condition. In addition, their shape resembles closely that obtained for polypyrrole films grown from solutions of Py in 0.1 M TBAP/MeCN, though the peaks are detected at higher potentials due to N-substitution [14]. Although the intensity of these peaks decreases with aging as the analyte bulkiness increases with hydrolysis, this factor determines

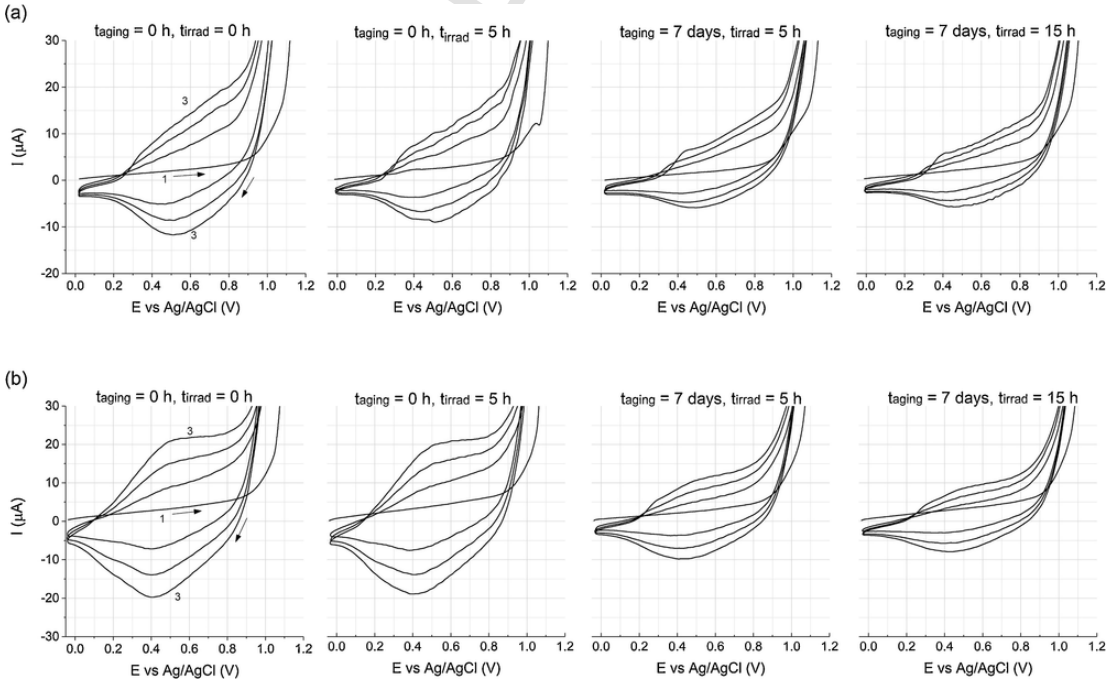

Fig. 5. Cyclic voltammograms ($\nu = 100$ mV/s, 0.1 M TBAP/ACN) recorded during electropolymerization of (a) N-PySi(MeOH), (b) N-PySi(MeOAc). Potential swept from 0.0 V to +1.2 V vs $Ag/AgCl/KCl_{(sat)}$ and then cycled 3 times between these potentials limits. The initial test conditions are indicated in the labels.

the extent of intramolecular polarization, the instauration of OH-π interactions and thus the contribution of different oligomeric domains, namely non-hydrolyzed and hydrolyzed α − α' linked Py oligomers, to the composition of the hybrid film. These observations are supported by the redox behavior of the films in monomer-free electrolyte solution (Fig. 6). The shoulder ascribed to TBA^+ uptake was always detected for N-PySi(MeOH) (Fig. 6a), while became distinguished with aging only in the case of N-PySi(MeOAc) (Fig. 6b). It is to be noticed that, with consecutive cycling, the current changes more significantly while two anodic and cathodic isopotential points at about +0.4 and +0.9 V become well defined, as obtained for the hybrid films electrodeposited using neat N-PySi monomer in 0.1 M TBAP/MeCN [14]. Non-hydrolyzed monomer or small oligomers within the hybrid network undergone irreversible processes associated to the acid-catalyzed hydrolysis of reactive methoxy groups by confined free protons of σ-oligomers intermediates.

The voltamograms recorded during electropolymerization of N-AnSi(MeOH) and N-AnSi(MeOAc) were closely similar, regardless t_{aging} and t_{irrad}. Representative voltammograms are reported in Fig. 7 for the case of AnSi(MeOH). An anodic peak at about +0.8 V was detected during the first anodic scan, while several reversible redox signals emerged at less positive potentials with subsequent potential cycling (Fig. 7, inset). The redox features reproduce rather well those obtained for neat N-AnSi monomer in 0.1 TBAP/MeCN (not shown) as well as those reported for unsubstituted polyaniline [21–23]. It is to be noticed that, differently from N-PySi (Fig. 5), the intensity of the oxidation

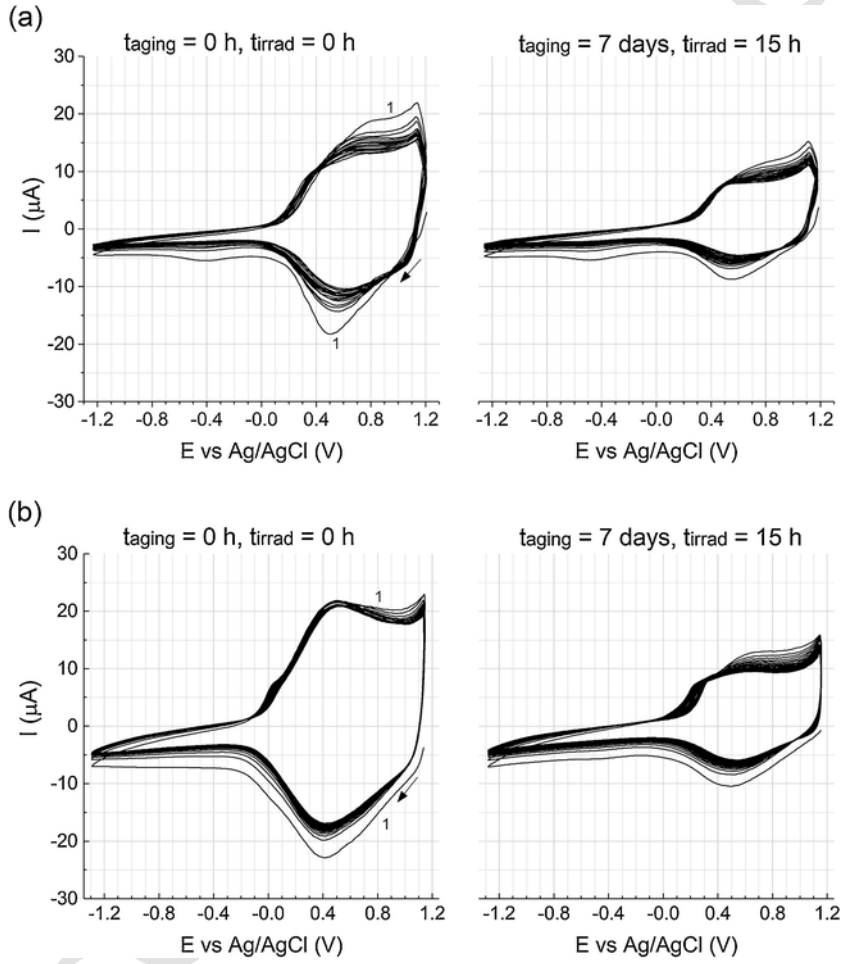

Fig. 6. Cyclic voltammograms ($\nu = 100$ mV/s) in analyte-free 0.1 M TBAP/MeCN of the electrodeposited hybrid films using (a) N-PySi(MeOH), (b) N-PySi(MeOAc). The starting conditions for the film growth (Fig. 5a,b) are indicated in the labels. Potential cycled between +1.2 and −1.2 V (15 times).

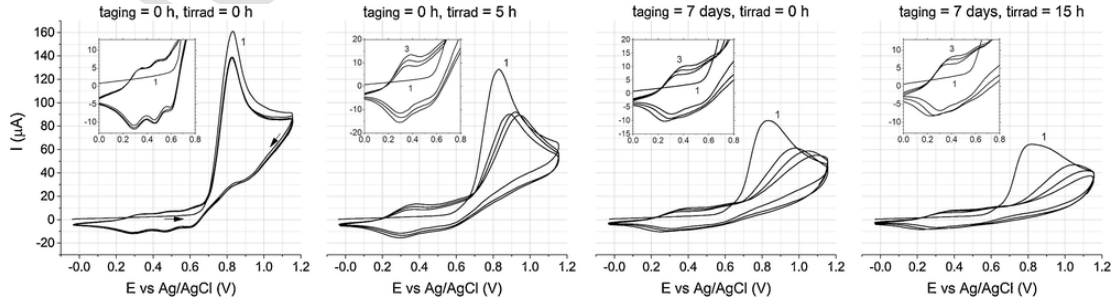

Fig. 7. Cyclic voltammograms ($\nu = 100$ mV/s, 0.1 M TBAP/ACN) recorded during electropolymerization of N-AnSi(MeOH). Potential swept from 0.0 V to +1.2 V vs Ag/AgCl/$KCl_{(sat)}$ and then cycled 3 times between these potentials limits. The initial test conditions are indicated in the labels.

peak was the only to decrease with the bulkiness of the analyte due to aging (Fig. 7), thus manifesting diffusion limitations due to the fast hydrolysis and self-condensation of SiOH. Steric effects that hinder the generation of rechargeable redox sites are less significant, according to the two redox couples at about +0.5 and +0.3 V related to the expulsion/uptake of H^+ and uptake/expulsion of ClO_4^-, respectively (Fig. 7, inset). The always well-defined reversible cation exchange conforms to the hindered acid-base reactions (emeraldine base EMB – emeraldine salt EMS transition) due to N-substitution [24,25]. However, the remaining more positive redox waves manifest reversible protonation/deprotonation with participation of semiquinoid aniline structures. The voltammograms of the hybrid films in monomer-free electrolyte solutions (Fig. 8) were very much dependent on both t_{aging}, t_{irrad} and the nature of the solvent in excess. More significantly, the shoulder preceding the anodic redox peak was better defined and stable with cycling for those conditions under which self-condensation of SiOH is less favored (Fig. 8, middle plots). Possible charge screening by SiOH due to entrapped within the hybrid network O···H—N complexes is supported by the decrease of the less positive reduction wave, manifesting irreversible expulsion of ClO_4^- into the electrolyte solution. Such screening became less effective with aging, according to the rapid decrease with consecutive potential cycling of the anodic shoulder, in particular for the case of aged AnSi(MeOH) (Fig. 8a, right). The macromolecular aggregation N-AnSi occurs through strong intermolecular hydrogen bonding rather than through cooperative though weaker dispersive van der Waals (vdW) interactions between silanol and the π system as in the case of N-PySi (Fig. 6) [13].

3.3. Electrochemical behavior of thiophenyl-silicon derivatives

The electropolymerization of unsubstituted thiophene (Tph) and of neat hybrid monomers α-ThpSi and β-ThpSi (Fig. 1c,d), as well as the redox behavior of the resulting films, were investigated as a start for reference purposes. Because thiophene has a higher oxidation potential (+1.7 V) in comparison to pyrrole and aniline, and possible n-doping could be detected at very negative potentials (≤ −1.25 V) [26], the anodic and cathodic potential limits used were higher (+1.8 and −2.0 V, respectively). Experiments using GC as working electrode showed worse defined redox waves, in particular for the case of α-ThpSi and β-ThpSi analytes. The results presented below correspond to experiments carried out with Pt disk (geometrical surface area of 0.7 cm^2, Ø = 3 mm, AMEL) as working electrode.

During the electropolymerization of Tph in 0.1 M TBAP/MeCN, the current increased importantly as the potential reached values near +1.5 V. Weak and broad cathodic and anodic redox peaks were detected at +0.5 and +1.3 V with subsequent potential cycling. The higher separation between the redox waves in comparison to that obtained for Py [14], as for N-PySi (Fig. 5), indicates irreversible discharging/charging of polythiophene due to more energetically stable interchain σ-dimeric intermediates [26]. During cycling of the electrodeposited film in monomer-free electrolyte (Fig. 9, curves 1), several redox features were detected, being the more negative cathodic peak ascribed to O_2 reduction as discriminated from the voltammogram of the background electrolyte and confirmed from experiments performed using Ar-saturated test solutions at different scan rates (Fig. 9, curves 2 and 3). Thus, the redox behavior of all the electrodeposited films was evaluated under Ar atmosphere by placing the gas inlet tube just above the liquid phase. The redox behavior of polythiophene points to at least two redox processes associated to different redox states and/or different mechanisms of charge transport. At E > 0.0 V, oxidation and reduction (p-doping) of regularly arranged oligothiophene chains is accompanied by the uptake and expulsion of electrolyte anions (ClO_4^-) for charge compensation. The better defined and more intense redox couple at E < 0.0 V manifests the prevalence of doping processes of opposite sign, namely n-doping involving reduction/oxidation of stable σ-coupled oligomeric chains [26,27]. Ion trapping due to incomplete removal of the true trapped positive charge rather than irreversible

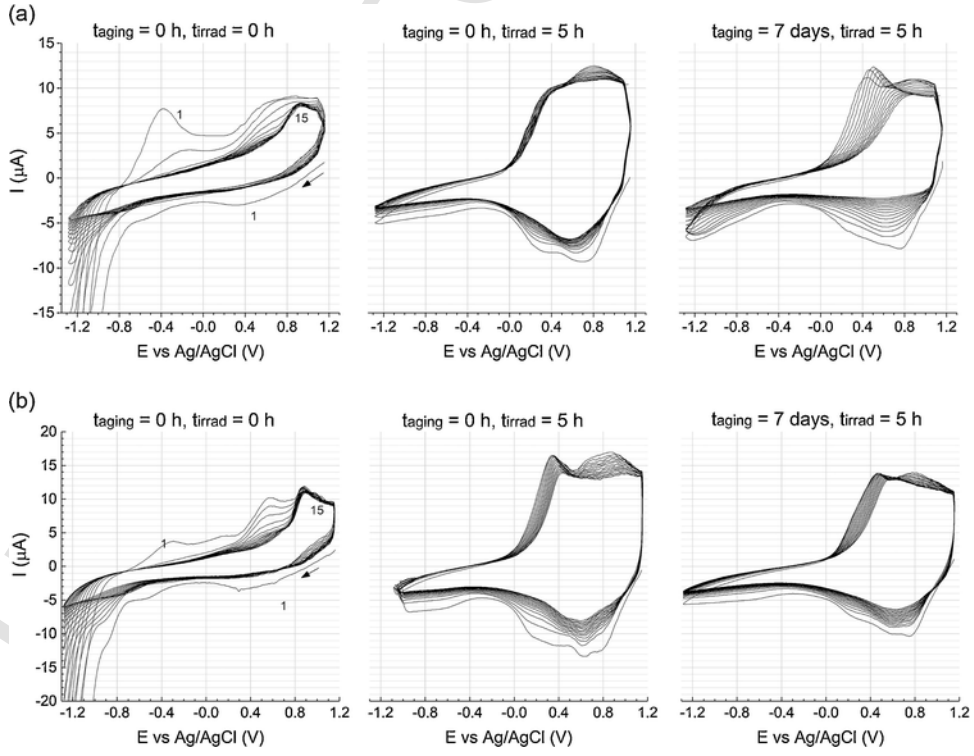

Fig. 8. Cyclic voltammograms (ν = 100 mV/s) in solute-free 0.1 M TBAP/MeCN of the electrodeposited films (Fig. 7a,b). The stating conditions (t_{aging} and t_{irrad}) are indicated in the labels. Potential cycled between +1.2 and −1.2 V (15 times).

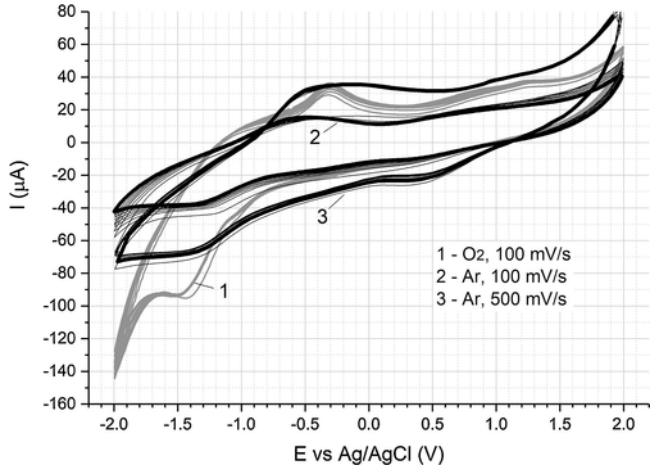

Fig. 9. Cyclic voltammograms of polythiophene films in naturally aerated and Ar-saturated monomer-free 0.1 M TBAP/MeCN.

chemical transformations is suggested by the widening of the conjugate n-doping bands as the scan rate is raised.

The oxidation peak of neat α-ThpSi and β-ThpSi in 0.1 M TBAP/MeCN was detected at less positive potentials (≈ + 1.4 V) in accordance with the facilitated Tph ring oxidation by the electron-donating alkyl side chain (inductive through-bond effect) [14,26]. However, the oxidation current decreased markedly after the first anodic scan for the case of α-ThpSi (Fig. 10a), also when a GC working electrode was used. The redox behavior of the resulting α-ThpSi was dominated by well-defined redox waves at E < 0.0 V (Fig. 10b), resembling those corresponding to n-doping of polythiophene (Fig. 9, curves 2,3). Conversely, the oxidation peak decreased progressively during electropolymerization of β-ThpSi by recurrent potential cycling while ill-defined p- and n-doping bands were recorded in monomer-free 0.1 M TBAP/MeCN. Differently from N-PySi (Fig. 6) [14], no solid state processes manifesting irreversible hydrolysis of methoxy groups by acidic σ-intermediates resulted evident in any case. By scrutiny with the redox behavior of polythiophene (Fig. 9, curves 2,3), highly disordered and polydispersive β-ThpSi film is formed due to favored α − α' linking but disfavored interchain σ-coupling by the shielding effect of the side chain. The dominating inductive effect over possible OH-π interactions was confirmed by the closely similar electrochemical behavior of β-ThpSi analyte in different solvent mixtures (200 μL in 0.1 TBAP/MeCN). For the case of α-ThpSi, stable σ-coupled dimers and hindered crosslinking reactions through α − β couplings by steric shielding of accessible redox states are likely to determine the n-type charge transport. In fact, no film but recurrent formation of pink colored species diffusing away from the electrode surface was observed during electropolymerization of α-ThpSi analyte in different solvent mixtures. The same was observed when GC as working electrode was used. The amount of colored species resulted more significant for α-ThpSi(MeOH), in correspondence with the more intense and the negligible variation of the irreversible anodic peak (≈ + 1.4 V) during consecutive cycling (Fig. 10c). More intense absorption bands at about 540 nm and 510 nm were detected in the Vis spectrum of the synthesis solution at the end of the electrochemical experiment. The prevalent formation of soluble pink species was confirmed from experiments using aged α-ThpSi (t_{aging} ≥3 days). The less intense and decreasing with consecutive cycling oxidation peak (Fig. 10d) manifests diffusion-limited charge transfer due to the promoted with hydrolysis/condensation analyte bulkiness. The results indicate that electrochemical oxidation of hydrolyzed α-ThpSi leads to α − α' linked dimer carbocations stabilized by OH-π interactions, in support to intramolecular polarization effects.

Spectroelectrochemical experiments were carried out to investigate the structure and stability of the soluble pink species, using as-prepared and aged up to 14 days α-ThpSi(MeOH). The results are summarized in Fig. 11. Preliminary potentiodynamic polarization experiments with

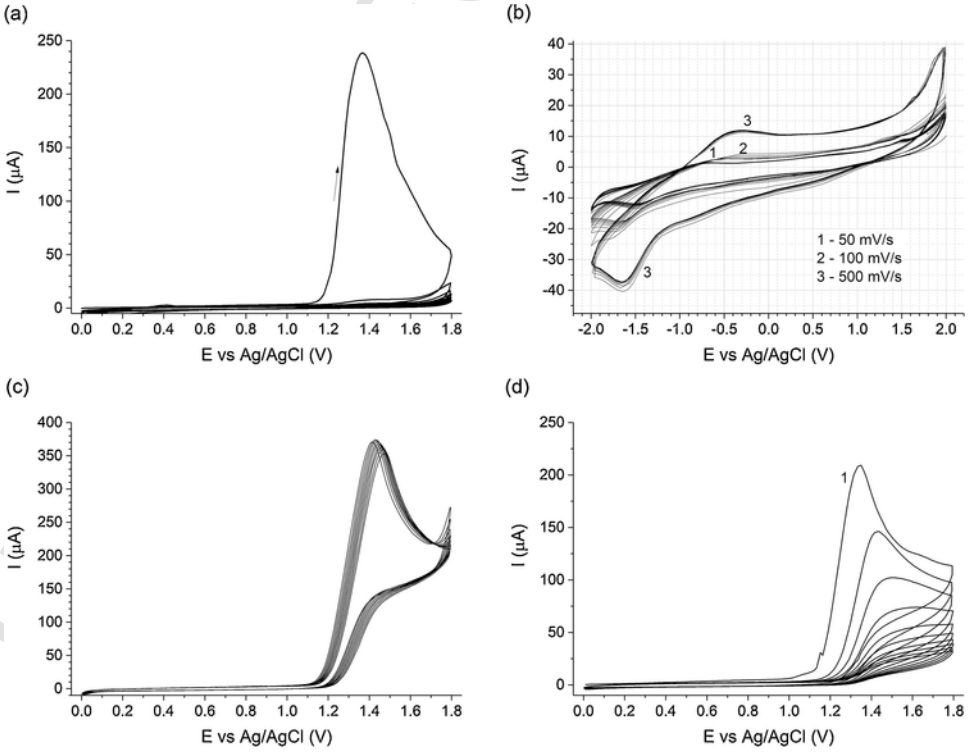

Fig. 10. (a) Cyclic voltammograms (100 mv/s) recorded during electropolymerization of α-ThpSi in 0.1 TBAP/MeCN; (b) Cyclic voltammograms at different scan rates of the electrodeposited film (a) in monomer-free 0.1 TBAP/MeCN; (c,d) Cyclic voltammograms recorded during electropolymerization of as-prepared and 10-days aged α-ThpSi(MeOH).

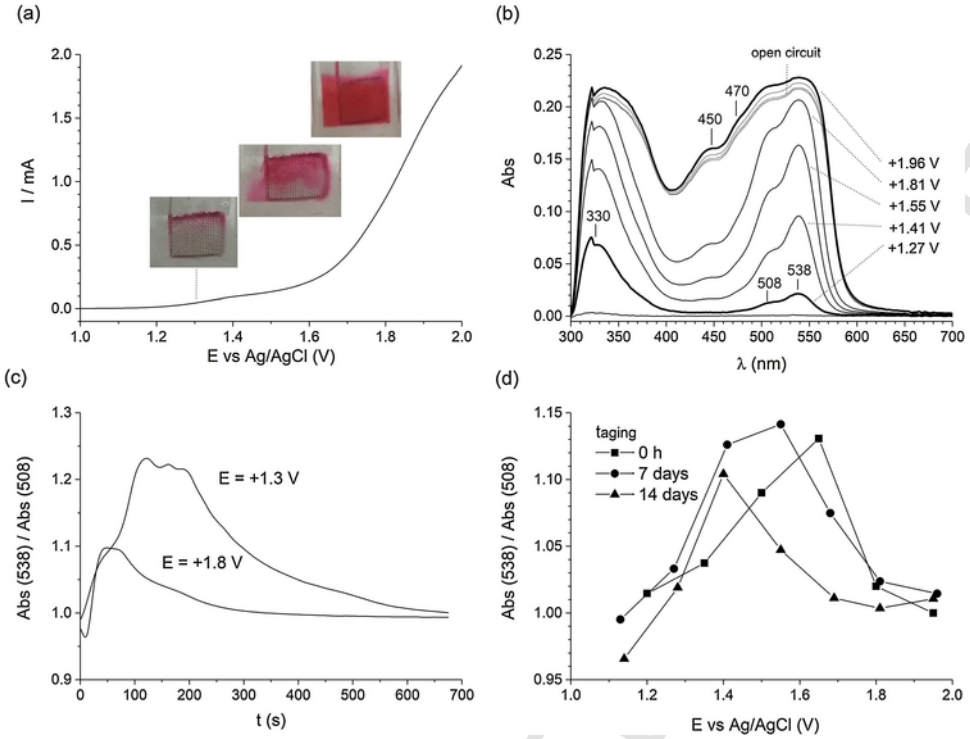

Fig. 11. (a) Potentiodynamic polarization curve (2 mV/s) during electropolymerization of α-ThpSi(MeOH) in the spectroelectrochemical cell containing 0.1 M TBAP/MeCN as supporting electrolyte. The images in the inset show the accumulation of pink-colored species in the vicinity of the Pt electrode with increasing anodic potential; (b) UV–vis spectra consecutively recorded during potentiodynamic polarization; (c) Variation of the ratio of the absorbance of the peaks at 508 and 538 nm as a function of time during potentiostatic polarization at +1.3 and +1.8 V; (d) Variation of the ratio of the absorbance of the peaks at 508 and 538 nm as a function of applied anodic potential of as-prepared and aged α-ThpSi(MeOH).

the spectroelectrochemical cell placed outside the spectrophotometer and containing the as-prepared α-ThpSi(MeOH) in 0.1 TBAP/MeCN confirmed the formation of pink colored products near the Pt mesh electrode in correspondence with the detection of a shoulder at +1.3 V in the I-E curve (Fig. 11a). Accumulation of these products rather than formation of larger oligomers was ascertained by the intensification of the pink coloration as the potential was made more positive. The discoloration of the synthesis solution was observed after about 10 min of experiment termination. The electrochemical response (Fig. 11a) was reproduced during the concomitant recording of the UV/Vis/NIR spectra. No peaks at $\lambda > 650$ nm but three bands at smaller wavelengths that increased in intensity with anodic polarization up to +1.8 V were confirmed after subtraction of the similarly recorded spectra of the analyte-free background electrolyte. As shown in Fig. 11b, the weak peak at 330 nm increases markedly in intensity while new bands at 508 and 535 nm appear as the anodic potential reaches values close to +1.3 V. These three bands present comparable absorbance values at $E > +1.5$ V. Shoulders at 450 and 470 nm are better defined for higher polarization potentials (between 1.8 and 2.0 V). Based on spectroscopic studies of thiophene and oligomers [26–32], fast coupling of monomeric radical cations of α-ThpSi (330 nm) produces α – α' ThpSi dimers that upon oxidation form dimeric (aromatic/quinoid) carbocations stabilized by intramolecular OH-π interactions (500–540 nm). At higher potentials possible crosslinking involving the free β-positions could occur, but higher oligomers are disfavored and no deposition processes occur (absence of bands at $\lambda > 650$ nm). The formation and the higher stability of aromatic/quinoid dimer species at less positive potentials was confirmed from absorbance measurements at 508 and 538 nm during potentiostatic polarization at +1.3 and +1.8 V (Fig. 11c). The results above (Fig. 11a,b) were reproduced for the case of aged α-ThpSi(MeOH). However, the intensity of the peaks at 508 and 538 nm increased more importantly up to 1.55 V while decreased more markedly as the applied potentials was made more positive. In addition, the 450-nm peak increased more importantly while that at 470 nm was hardly resolved with anodic polarization. Fig. 11d graphically summarizes the variation of the former two peaks, expressed as the ratio between the absorbance of the 538- and 508-nm peaks for a given aging condition and plotted as a function of the applied potential. The availability of donor – acceptor hydrolyzed monomer units that are expected to have smaller band gap, in similarity to N-PySi [13], increases with hydrolysis and thus the formation of dimeric structures is more favored. However, the stability of the latter species is compromised by hydrogen bonding/condensation between SiOH groups. Thus, short-range intramolecular mechanism is likely to account for the effectiveness of the OH-π interactions in the case of the α-substituted thiophenyl-silicon derivative. It is worth mentioning that soluble but colorless oligomers of α-substituted thiophene with trimethylsilyl groups (—Si—$(CH_3)_3$) have been reported [29].

The significance of OH-π intramolecular interactions is strengthened by the fact that, differently from β-ThpSi which stock solutions developed whitish and/or brownish precipitates with prolonged aging, colored gels were obtained for the case of α-ThpSi, also in different solvent systems like pure MeCN and this containing 1 vol.% of H_2O. Purple gels were formed in all cases but MeOAc (yellow gel), being the color more intense in the case of α-ThpSi(MeCN) and α-ThpSi(MeOH). From the comparison of the attenuated total reflection infrared (ATR-IR) spectra of the purple α-ThpSi(MeOH) and yellow α-ThpSi(MeOAc) gels (Fig. 12), the former shows a more intense broad band between 3600 and 3200 cm^{-1}. Although the associated OH stretching vibration (ν_{OH}) could result from the MeOH entrapped in the gel phase, the more intense shoulder at about 3260 cm^{-1} and the less intense peak at about 1010 cm^{-1} of SiOH deformation (δ_{SiOH}) correlate with the features of intermolecular hydrogen-bonded network [33]. In addition, hindered motions of alkyl side chain due to internal, three-dimensionally more

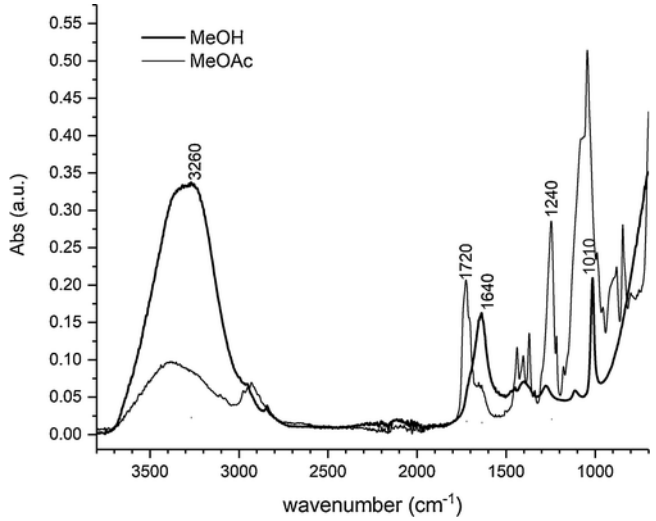

Fig. 12. ATR-IR spectra of the purple and pale yellow gels formed with aging (two months) of α-ThpSi(MeOH) and α-ThpSi (MeOAc) solutions. Spectra recorded with a Nicolet 380 FT-IR instrument in the frequency range 3800–700 cm^{-1} (98% sensitivity) using Zn–Se crystal.

rigid gel phase is indicated by the absence of peaks between 930 and 850 cm^{-1} (rocking and twisting deformation modes). Also, much more intense and broad is the peak at 1640 cm^{-1} corresponding to the C═C stretching ($\nu_{C=C}$) of the aromatic Thp ring. For the case of the yellow α-ThpSi(MeOAc) gel, entrapped solvent is indicated by the intense and sharp peaks at 1720 and 1240 cm^{-1} associated to C═O ($\nu_{C=O}$) and C—O (ν_{C-O}) stretching vibrations. The intense Si-O—C peaks between 1150 and 1000 cm^{-1} manifest the presence of non-hydrolyzed structures, providing confirmation of less favored hydrolysis in the presence of MeOAc in excess. Formation of saturated carbonyl compounds, probably acetylthiophene (pale yellow-colored), is suggested by the intense shoulder at 1700 cm^{-1}.

Additional experiments were carried out to investigate the redox behavior of the above mentioned purple gels. The Pt electrode was immersed in 2 mL of $CHCl_3$ into which a given amount of gel was dissolved and left overnight for solvent evaporation. A pink patina covering the electrode surface was observed at naked eyes. Cyclic voltammograms were recorded in monomer-free 0.1 TBAP/MeCN using −1 V as cathodic limit in order to avoid the detachment of the gel film. The characteristic n-doping charging/discharging behavior involving a peak-shaped reduction wave and a current plateau during cathodic reduction [26] is obtained for the case of α-ThpSi(MeOH) gel only (Fig. 13a). This definitely confirms that OH-π interactions through a short-range intramolecular mechanism promote stabilization and charge trapping of hydrolyzed σ-dimers of α-ThpSi. Furthermore, the development of colored gels in the case of α-ThpSi(MeCN) and α-ThpSi(MeCN, 1 vol% H_2O), supports the instauration of OH-π interactions due to irreversible chemical reactions between reactive methoxy groups and acidic σ-dimeric intermediates, as indicated from the electrochemical experiments with N-PySi (Fig. 6) [14]. Note that hydrolysis reactions should be more favored in MeCN, which is aprotic but more polar than MeOAc. Nonetheless, the broad reduction wave detected at about 0.0 V (Fig. 13b) points to facilitated proton elimination and rearomatization of σ-dimers [26], and thus less stable OH-π aggregates. In addition, the absence of redox features at $E < 0.0$ V and the important decrease with consecutive cycling of the several oxidation bands at $E > 0.0$ V manifest less effective charge trapping due to restricted hydrogen-bonding oligomerization and unstable p-doping due to restricted π-conjugation. Recall of corrosion experiments with chemically-modified steel surfaces using α-substituted thiophenylthio derivative (Fig. 2c,d), the expected n-type redox behavior, being supported further by the higher resonance stability due to the thio group at Cα, would justify the significant inhibition of the undermining substrate degradation.

4. Conclusions

Monomers of conducting polymers such as aniline, pyrrole and thiophene substituted with methoxysilyl propyl end groups were investigated as a function of the extent of hydrolysis and of the ex-situ photo-oxidation by spectroscopic and electrochemical techniques. The interactions between the silanol end groups and the aromatic π system rather than the oligomerization promoted with either photo-oxidation or electrochemical oxidation of the monomer head group determine the extent of charge trapping and thus the n-type redox behavior of the electrogenerated hybrid networks. The cooperative contribution of long-range OH-π interactions accounting for the mixed n-p doping redox behavior of hybrid N-PySi agglomerates is confirmed. Less powerful are the donor-acceptor interactions for the case of N-AnSi due to the more basic character of this monomer promoting deprotonation and self-condensation of SiOH, thus prevailing a p-type charge transport mechanism as for contiguous polyaniline. The n-doping behavior upon jellification of the hydrolyzed α-ThpSi derivative confirms that short-range intramolecular OH-π interactions operate for the stabilization of soluble σ-dimeric hydrolyzed structures. The differences above are impelled by the stability of the electrogenerated carbocations of hydrolyzed monomers. The n-type redox properties indicated for N-PySi and α-ThpSi hydrolyzed precursors support the higher barrier action against corrosion provided by the resulting thin hybrid films, limiting both O_2 reduction and Cl^- attack at the metal/film interface. Present findings provide further evidence on the modulation of the physico-chemical properties of macromolecular architectures through chemical functionalization of silicon-based building blocks. The new insights for

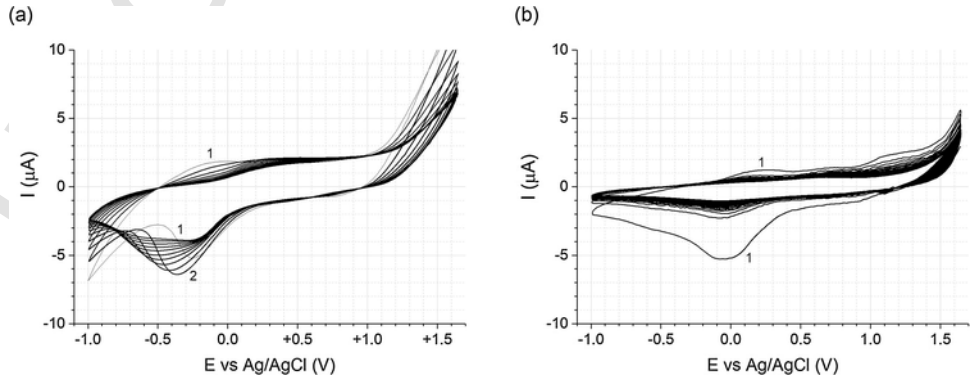

Fig. 13. Cyclic voltammograms (ν = 100 mV/s, 0.1 M TBAP/MeCN) of the gel films obtained from aged α-TphSi in (a) MeOH:H_2O (90:10); (b) MeCN containing 1vol% H_2O.

the design of advanced coatings are not limited to solid state films for protection of reactive metals but may be extended to electroresponsive hydrogels that are of much concern to hydrogel science for applications in nanotechnology and biomedicine, where materials degradation is an important issue also.

Acknowledgements

The authors wish to thanks Prof. M. Benaglia (Department of Chemistry, Università degli Studi di Milano) for the facilities and guidance in the synthesis of β-ThpSi. The use of UV–vis-NIR spectrometer purchased through the Regione Lombardia – Fondazione Cariplo joint SmartMatLab Project (Fondazione Cariplo grant 2013-1766) is gratefully acknowledged.

Appendix A. Supplementary data

Supplementary data associated with this article can be found, in the online version, at https://doi.org/10.1016/j.porgcoat.2018.05.010.

References

[1] H. Wang, V. Kumara, Transparent and conductive polysiloxanes/PEDOT:PSS nanocomposite thin films with a water-impermeable property to significantly enhance stability of organic–inorganic hybrid solar cells, RSC Adv. 5 (2015) 9650–9657.
[2] J. Rivnay, R.M. Owens, G.G. Malliaras, The rise of organic bioelectronics, Chem. Mater. 26 (2014) 679–685.
[3] M. Karakoy, E. Gultepe, S. Pandey, M.A. Khashab, D.H. Gracias, Silane surface modification for improved bioadhesion of esophageal stents, Appl. Surf. Sci. 311 (2014) 684–689.
[4] M. Ammar, C. Smadja, G.T.P. Ly, D. Tandjigora, J. Vigneron, A. Etcheberry, M. Taverna, E. Dufour-Gergam, Chemical engineering of self-assembled Alzheimer's peptide on a silanized silicon surface, Langmuir 30 (2014) 5863–5872.
[5] U.G. Spizzirri, M. Curcio, G. Cirillo, T. Spataro, O. Vittorio, N. Picci, S. Hampel, F. Iemma, F.P. Nicoletta, Recent advances in the synthesis and biomedical applications of nanocomposite hydrogels, Pharmaceutics 7 (2015) 413–437.
[6] A. Mirabedini, J. Foroughi, G.G. Wallace, Developments in conducting polymer fibres: from established spinning methods toward advanced applications, RSC Adv. 6 (2016) 44687–44716.
[7] M.F. Montemor, Functional and smart coatings for corrosion protection: a review of recent advances, Surf. Coat. Technol. 258 (2014) 17–37.
[8] (a) M. Trueba, S.P. Trasatti, Pyrrole-based silane primer for corrosion protection of commercial Al alloys. Part I: synthesis and spectroscopic characterization, Prog. Org. Coat. 66 (2009) 254–264.
[9] M. Trueba, S.P. Trasatti, D.O. Flamini, Hybrid coatings based on conducting polymers and polysiloxane chains for corrosion protection of Al alloys, Adv. Mater. Res. 138 (2010) 63–78.
[10] D.O. Flamini, M. Trueba, S.P. Trasatti, Aniline-based silane as a primer for corrosion inhibition of aluminium, Prog. Org. Coat. 74 (2012) 302–310.
[11] M. Trueba, S.P. Trasatti, D.O. Flamini, The effect of aluminium alloy secondary phases on aniline-based silane protection capacity, Corros. Sci. 63 (2012) 59–70.
[12] S. Bianchi, M. Trueba, S.P. Trasatti, E. Madaschi, M.C. Sala, An in-depth comprehension of the protection mechanism of Al alloys by aniline-based silane, Prog. Org. Coat. 77 (2014) 2054–2065.
[13] S. González-Santana, C. Morera-Boado, L.A. Montero-Cabrera, M. Trueba, S.P. Trasatti, Pyrrolyl-silicon compounds as precursors for donor-acceptor systems stabilized by noncovalent interactions, J. Phys. Chem. A 119 (2015) 7038–7051.
[14] E. Volpi, L. Falciola, M. Trueba, S.P. Trasatti, M.C. Sala, E. Pini, A. Contini, Pyrrolyl-silicon compounds with different alkyl spacer lengths: synthesis, electrochemical behavior and binding properties, Synth. Met. 231 (2017) 127–136.
[15] C.M. Santi, G. Conchetto, M. Trueba, S.P. Trasatti, Electrochemical characterization of organofunctionalized silanes as precursor for surface treatments, Metallurgia Ital. 109 (2017) 19–22.
[16] P. Geysermans, F. Finocchi, J. Goniakowski, R. Hacquart, J. Jupille, Combination of (100), (110) and (111) facets in MgO crystals shapes from dry to wet environment, Phys. Chem. Chem. Phys. 11 (2009) 2228–2233.
[17] X. Wu, T. Chen, L. Zhu, R.D. Rieke, Room-temperature stable 3-lithiothiophene – a facile synthesis of 3-functional thiophenes, Tetrahedron Lett. 35 (1994) 3673–3674.
[18] G. Gritzner, Reference redox systems in nonaqueous systems and the relation of electrode potentials in nonaqueous and mixed solvents to standard potentials in water, in: G. Inzelt, A. Lewenstam, F. Scholz (Eds.), Handbook of Reference Electrodes, Springer, Berlin, Heidelberg, 2013, pp. 25–31, https://doi.org/10.1007/978-3-642-36188-3_2, (Ch. 2).
[19] S. Okur, U. Salzner, Theoretical modeling of the doping process in polypyrrole by calculating UV/Vis absorption spectra of neutral and charged oligomers, J. Phys. Chem. A 112 (2008) 11842–11853.
[20] H.S. Nalwa (Ed.), Handbook of Advanced Electronic and Photonic Materials and Devices, Vol. 8, Conducting Polymers, Academic press, Harcourt Science and Technology Company, San Diego, USA, 2001.
[21] F. Wudl, R.0 Angus, Jr., F.L. Lu, P.M. Allemand, D.J. Vachon, M. Nowak, Z.X. Liu, A.J. Heeger, Poly(p-phenyleneamineimine). Synthesis and comparison to polyaniline, J. Am. Chem. Soc. 109 (1987) 3677–3684.
[22] H. Yang, A.J. Bard, The application of fast scan cyclic voltammetry. Mechanistic study of the initial stage of electropolymerization of aniline in aqueous solutions, J. Electroanal. Chem. 339 (1992) 423–449.
[23] T.F. Otero, I. Boyano, Potentiostatic oxidation of polyaniline under conformational re-laxation control: experimental and theoretical Study, J. Phys. Chem. B 107 (2003) 4269–4276.
[24] T. Lindfors, A. Ivaska, pH sensitivity of polyaniline and its substituted derivatives, J. Electroanal. Chem. 531 (2002) 43–52.
[25] T. Lindfors, A. Ivaska, Potentiometric and UV–vis characterisation of N-substituted polyanilines, J. Electroanal. Chem. 535 (2002) 65–74.
[26] J. Heinze, B.A. Frontana-Uribe, S. Ludwigs, Electrochemistry of conducting polymers – persistent models and new concepts, Chem. Rev. 110 (2010) 4724–4771.
[27] O.A. Semenikhin, E.V. Ovsyannikova, M.R. Ehrenburg, N.M. Alpatova, V.E. Kazarinov, Electrochemical and photoelectrochemical behaviour of polythiophenes in non-aqueous solutions Part 2. The effect of charge trapping, Electroanal. Chem. 494 (2000) 1–11.
[28] M.G. Hill, J.-F. Penneau, B. Zinger, K.R. Mann, L.L. Miller, Oligothiophene cation radicals. π-Dimers as alternatives to bipolarons in oxidized polythiophenes, Chem. Muter. 4 (1992) 1106–1113.
[29] J.M. Tour, R. Wu, Synthesis and UV-Visible properties of soluble α-thiophene oligomers. Monomer to Octamer, Macromolecules 25 (1992) 1901–1907.
[30] W.-C. Chen, S.A. Jenekhe, Small-bandgap conducting polymers based on conjugated poly(heteroary1ene methines. 2. Synthesis, structure, and properties, Macromolecules 28 (1995) 465–480.
[31] A. Smie, A. Synowczyk, J. Heinze, R. Alle, P. Tschuncky, G. Götz, P. Bäuerle, β,β-disubstituted oligothiophenes, a new oligomeric approach towards the synthesis of conducting polymers, J. Electroanal. Chem. 452 (1998) 87–95.
[32] J. Heinze, H. John, M. Dietrich, P. Tschuncky, σ-Dimers – key intermediates and products during generation and redox switching of conjugated oligomers and polymers, Synth. Met. 119 (2001) 49–52.
[33] M. Montejo, F. Partal Ureña, F. Márquez, J.J. López González, Triethylsilanol Molecular conformations and role of the hydrogen-bonding oligomerization in its vibrational spectra, J. Phys. Chem. A 112 (2008) 1545–1551.